Natural Hazards
and Earth System
Sciences

Open Access

Supplement of

Analysing the spatial patterns of erosion scars using point process theory at the coastal chalk cliff of Mesnil-Val, Normandy, northern France

J. Rohmer and T. Dewez

Correspondence to: J. Rohmer (j.rohmer@brgm.fr)

Figure 1S. Lurking variable plots for the winter 2006 displaying the point process residuals (cumulative raw) under the assumption of Complete Spatial Randomness against the *x*-coordinate (alongshore) and the *y*- coordinate (along cliff elevation) for small erosion scars (A and C), and for large erosion scars (B and D). The empirical plot (solid lines) is shown together with the pointwise two-standard-deviation limits (red lines).

Figure 2S. Lurking variable plots for the winter 2007 displaying the point process residuals (cumulative raw) under the assumption of Complete Spatial Randomness against the *x*-coordinate (alongshore) and the *y*- coordinate (along cliff elevation) for small erosion scars (A and C), and for large erosion scars (B and D). The empirical plot (solid lines) is shown together with the pointwise two-standard-deviation limits (red lines).

Figure 3S. Lurking variable plots for the summer 2007 displaying the point process residuals (cumulative raw) under the assumption of Complete Spatial Randomness against the *x*-coordinate (alongshore) and the *y*- coordinate (along cliff elevation) for small erosion scars (A and C), and for large erosion scars (B and D). The empirical plot (solid lines) is shown together with the pointwise two-standard-deviation limits (red lines).

Figure 4S. Lurking variable plots for the winter 2008 displaying the point process residuals (cumulative raw) under the assumption of a non sationary Poisson Process with linear trend along *x* and *y* for small erosion scars (A and C), and for large erosion scars (B and D). The empirical plot (solid lines) is shown together with the pointwise two-standard-deviation limits (red lines).

Figure 5S. Lurking variable plots for the summer 2007 displaying the point process residuals (cumulative raw) under the assumption of a non sationary Poisson Process with linear trend along *x* and *y* for small erosion scars (A and C), and for large erosion scars (B and D). The empirical plot (solid lines) is shown together with the pointwise two-standard-deviation limits (red lines).

Figure 6S. Empirical inhomogeneous *L*- function (minus the distance *r*) calculted for winter 2007 dataset with Ripley's edge correction (black-colored lines): for the small erosion scars, A) ($10^{-3} \leq$ volume $\leq 10^{-2}$ m^3) and for the large scars B) ($10^{-2} \leq$ volume $\leq 10^{1}$ m^3). The limits of confidence envelope (calculated through a Monte-Carlo procedure) at level of 2% are depicted by red curves.

Figure 7S. Empirical inhomogeneous *L*- function (minus the distance *r*) calculted for winter 2008 dataset with Ripley's edge correction (black-colored lines): for the small erosion scars, A) ($10^{-3} \leq$ volume $\leq 10^{-2}$ m^3) and for the large scars B) ($10^{-2} \leq$ volume $\leq 10^{1}$ m^3). The limits of confidence envelope (calculated through a Monte-Carlo procedure) at level of 2% are depicted by red curves.

Figure 8S. Cross-type L- functions computed between subsequent epochs of measurement (black-colored lines) considering the small erosion scars. The limits of confidence envelope at level of 2% associated to the "population independence" hypothesis are calculated considering 99 random shifts in a rectangular window of a 2.5 m x 2.5 m.

Figure 9S. Cross-type L- functions computed between subsequent epochs of measurement (black-coloured lines) considering the small erosion scars. The limits of confidence envelope at level of 2% associated to the "population independence" hypothesis are calculated considering 99 random shifts in a rectangular window of a 10 m x 10 m.

Figure 10S. Cross-type L- functions computed between subsequent epochs of measurement in winter (black-coloured lines) considering the large erosion scars. Figures C and D respectively correspond to a zoom on the distance range from 0 to 1.0 of Figures A and B. The limits of confidence envelope at level of 2% associated to the "population independence" hypothesis are calculated considering 99 random shifts in a rectangular window of a 2.5 m x 2.5 m.

Figure 11S. Cross-type L- functions computed between subsequent epochs of measurement in winter (black-coloured lines) considering the large erosion scars. Figures C and D respectively correspond to a zoom on the distance range from 0 to 1.0 of Figures A and B. The limits of confidence envelope at level of 2% associated to the "population independence" hypothesis are calculated considering 99 random shifts in a rectangular window of a 10 m x 10 m.
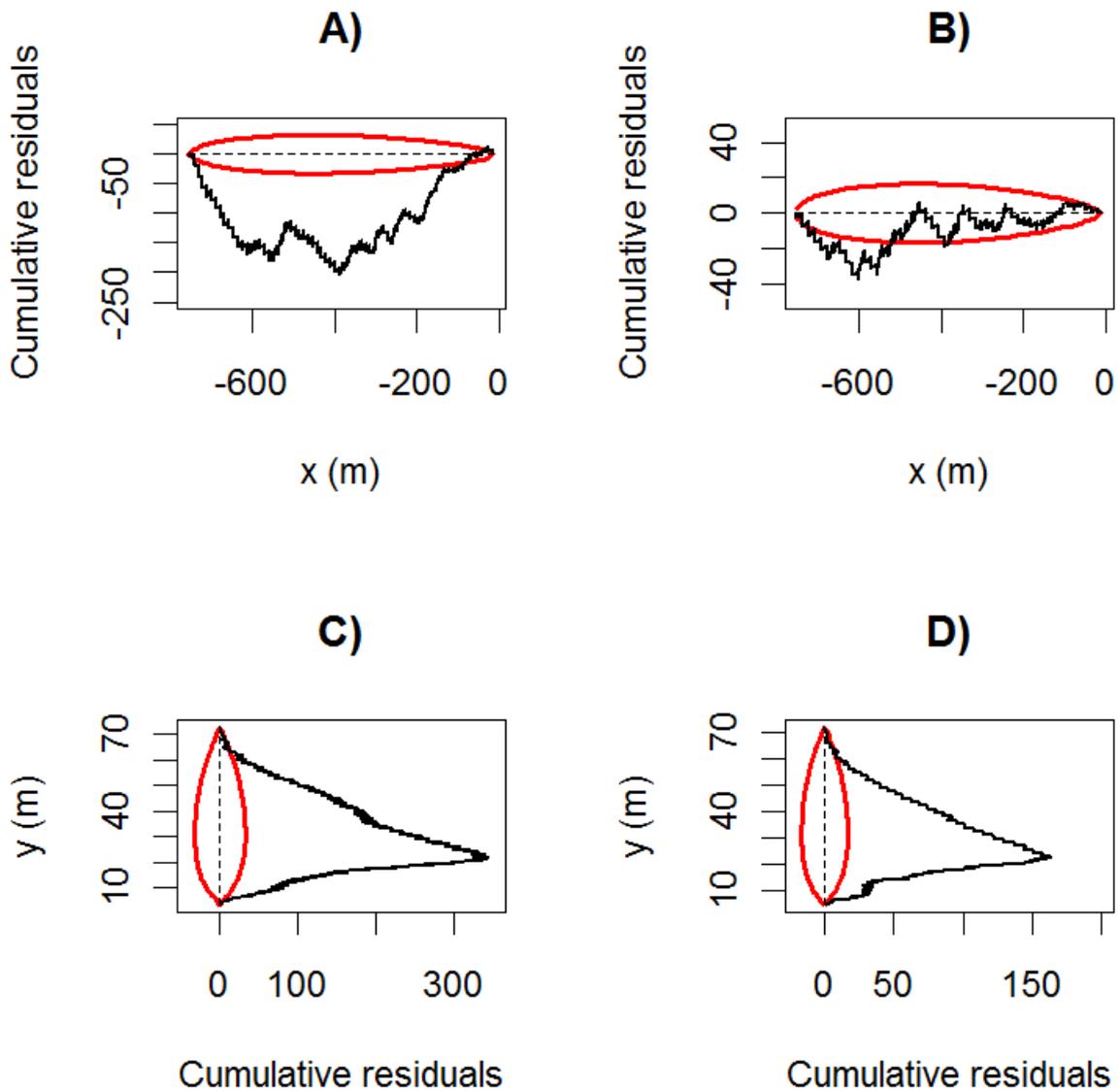
Figure 1S. Lurking variable plots for the winter 2006 displaying the point process residuals (cumulative raw) under the assumption of Complete Spatial Randomness against the *x*-coordinate (alongshore) and the *y*- coordinate (along cliff elevation) for small erosion scars (A and C), and for large erosion scars (B and D). The empirical plot (solid lines) is shown together with the pointwise two-standard-deviation limits (red lines).
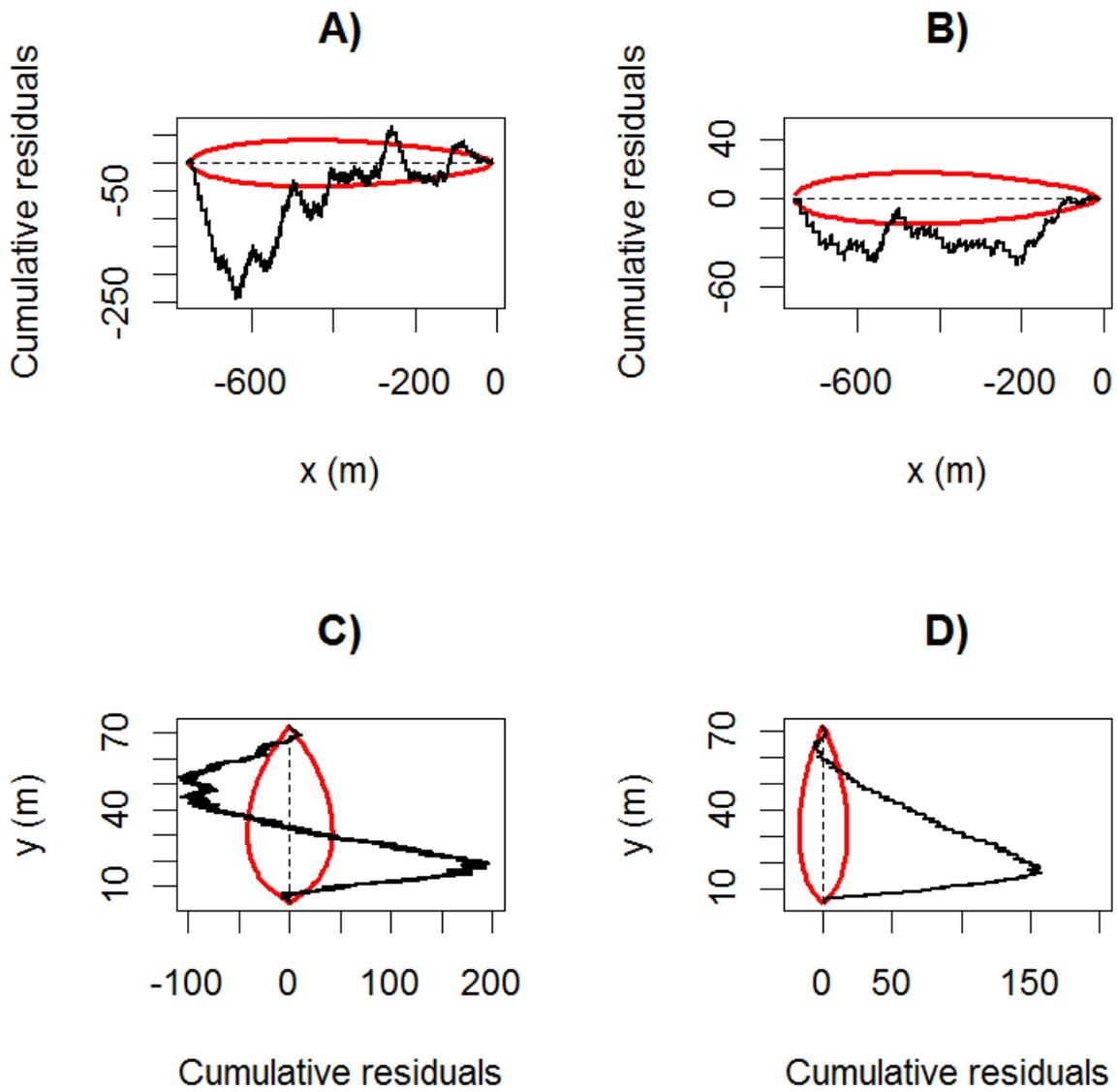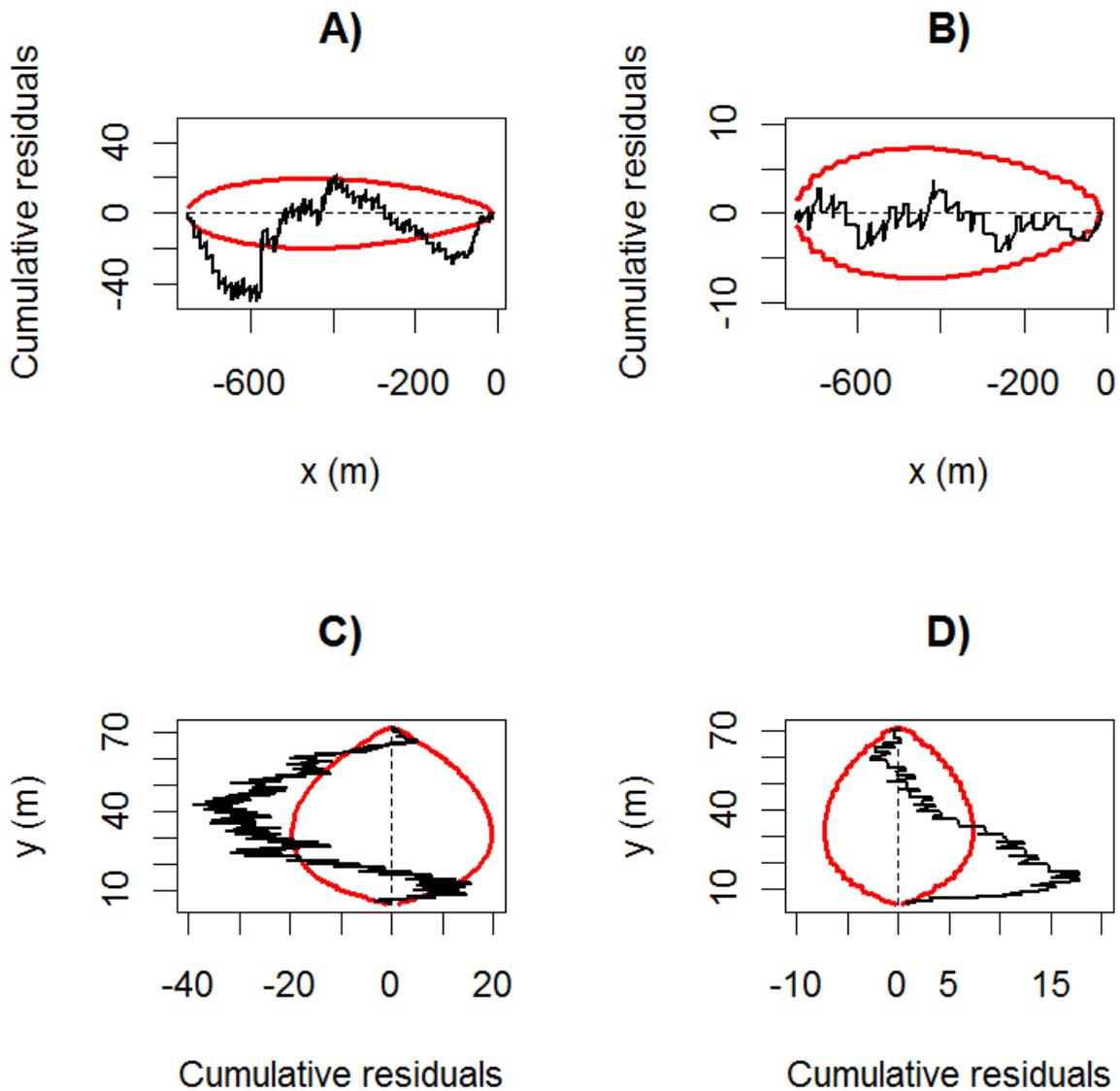
Figure 2S. Lurking variable plots for the winter 2007 displaying the point process residuals (cumulative raw) under the assumption of Complete Spatial Randomness against the *x*-coordinate (alongshore) and the *y*- coordinate (along cliff elevation) for small erosion scars (A and C), and for large erosion scars (B and D). The empirical plot (solid lines) is shown together with the pointwise two-standard-deviation limits (red lines).
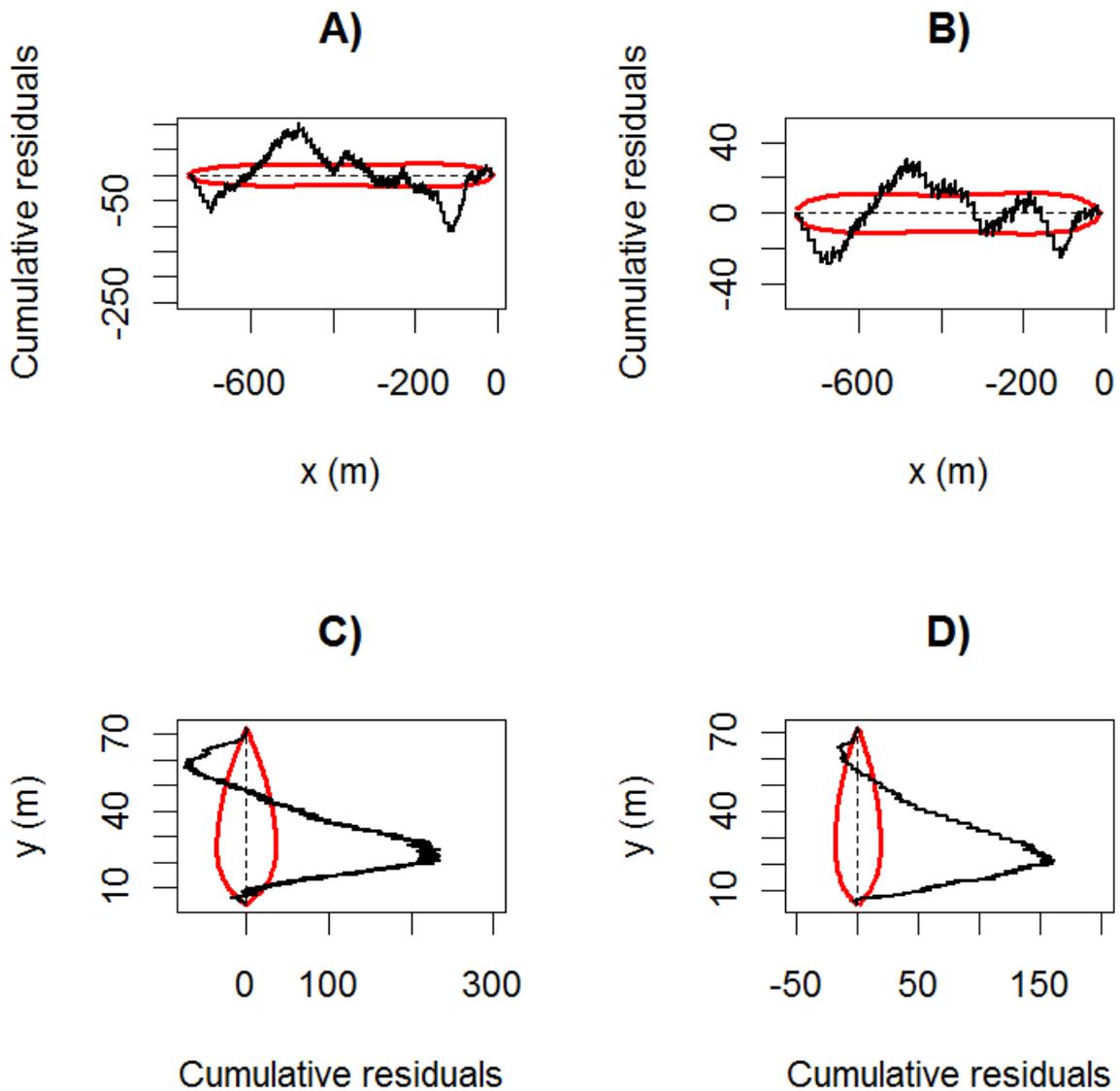
Figure 3S. Lurking variable plots for the summer 2007 displaying the point process residuals (cumulative raw) under the assumption of Complete Spatial Randomness against the *x*-coordinate (alongshore) and the *y*- coordinate (along cliff elevation) for small erosion scars (A and C), and for large erosion scars (B and D). The empirical plot (solid lines) is shown together with the pointwise two-standard-deviation limits (red lines).
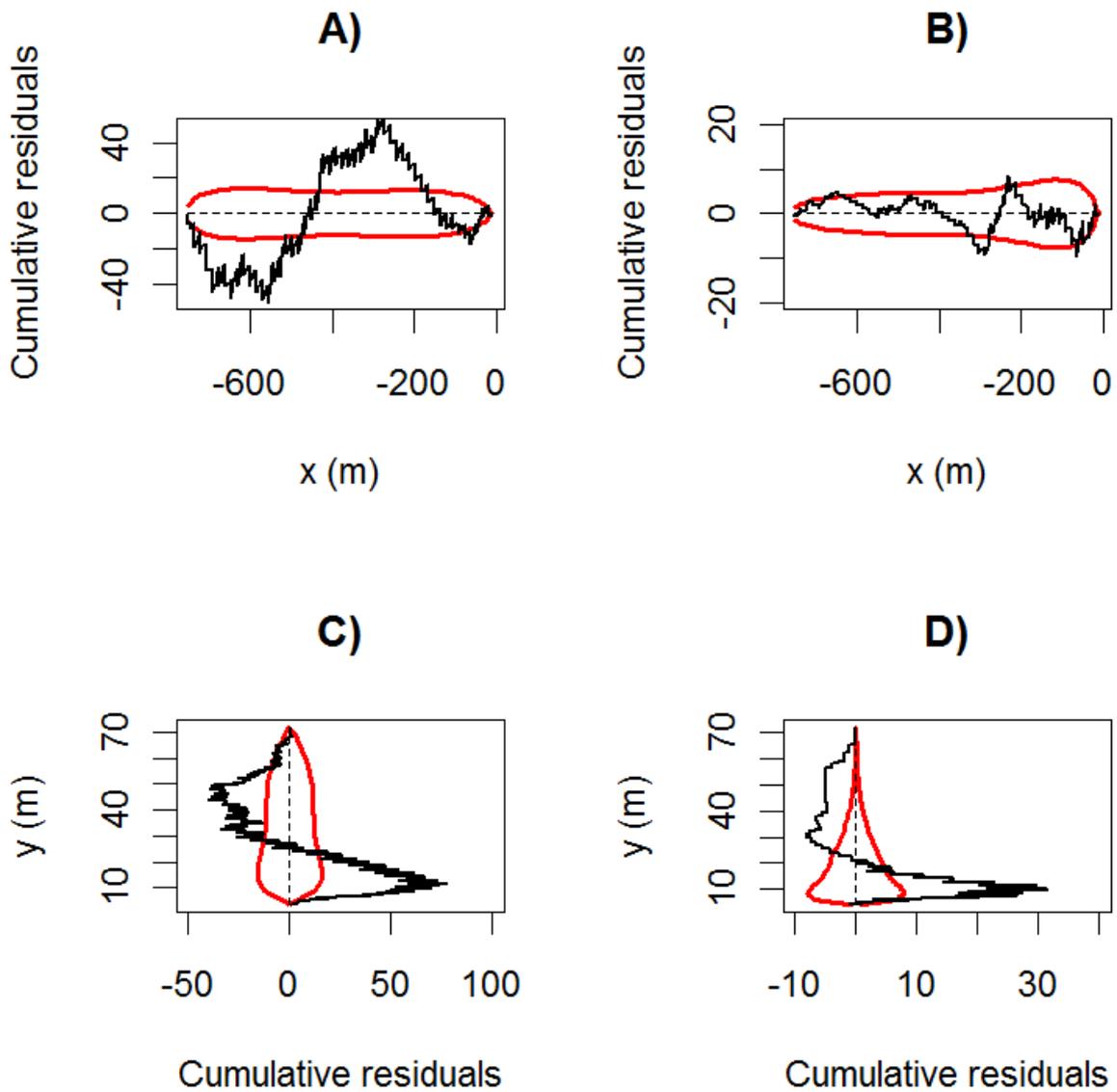
Figure 4S. Lurking variable plots for the winter 2008 displaying the point process residuals (cumulative raw) under the assumption of a non sationary Poisson Process with a spatial trend described by Eq. 6 for small erosion scars (A and C), and for large erosion scars (B and D). The empirical plot (solid lines) is shown together with the pointwise two-standard-deviation limits (red lines).
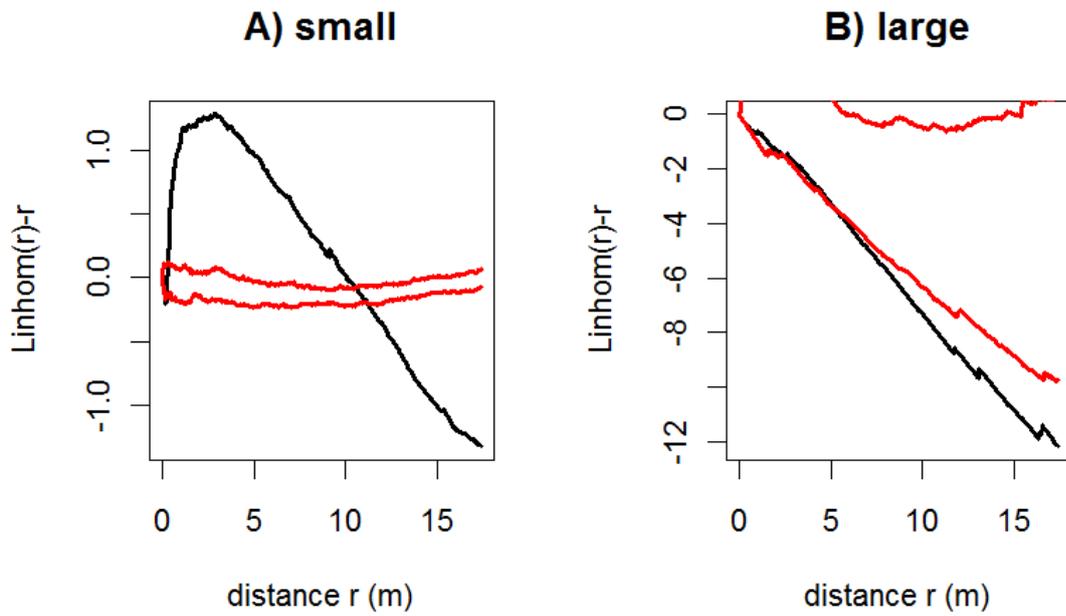
Figure 5S. Lurking variable plots (epoch of measurement: summer 2007) displaying the point process residuals (cumulative raw) under the assumption of a non sationary Poisson Process with a spatial trend described by Eq. 6 for small erosion scars (A and C), and for large erosion scars (B and D). The empirical plot (solid lines) is shown together with the pointwise two-standard-deviation limits (red lines).
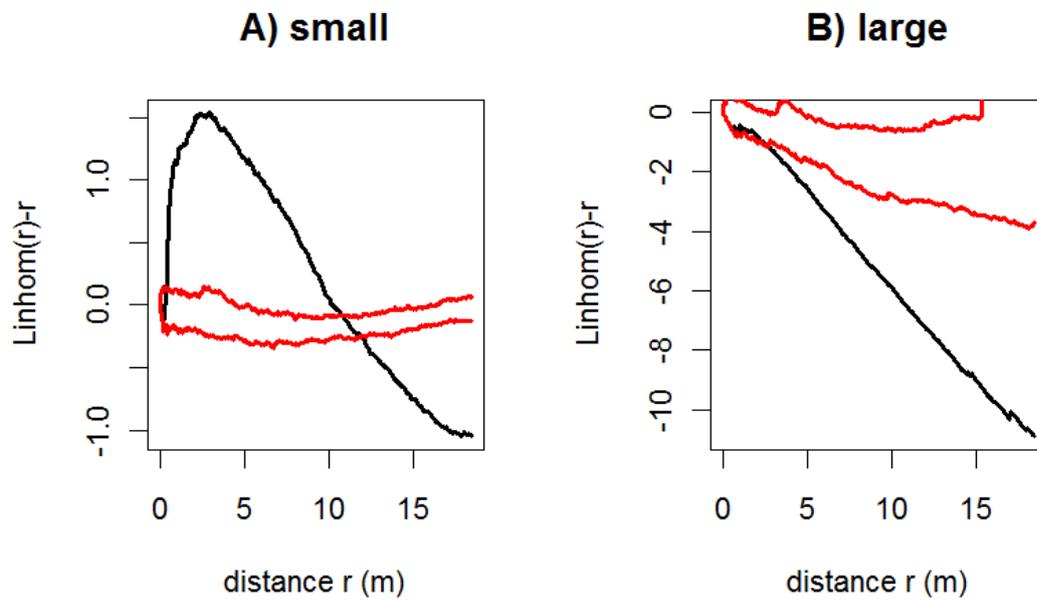
Figure 6S. Empirical inhomogeneous *L*- function (minus the distance *r*) calculted for winter 2007 dataset with Ripley's edge correction (black-colored lines): for the small erosion scars, A) ($10^{-3} \leq$ volume $\leq 10^{-2}$ m^3) and for the large scars B) ($10^{-2} \leq$ volume $\leq 10^{1}$ m^3). The limits of confidence envelope (calculated through a Monte-Carlo procedure) at level of 2% are depicted by red curves.

Figure 7S. Empirical inhomogeneous *L*- function (minus the distance *r*) calculted for winter 2008 dataset with Ripley's edge correction (black-colored lines): for the small erosion scars, A) ($10^{-3} \leq volume \leq 10^{-2}$ m^3) and for the large scars B) ($10^{-2} \leq volume \leq 10^{1}$ m^3). The limits of confidence envelope (calculated through a Monte-Carlo procedure) at level of 2% are depicted by red curves.
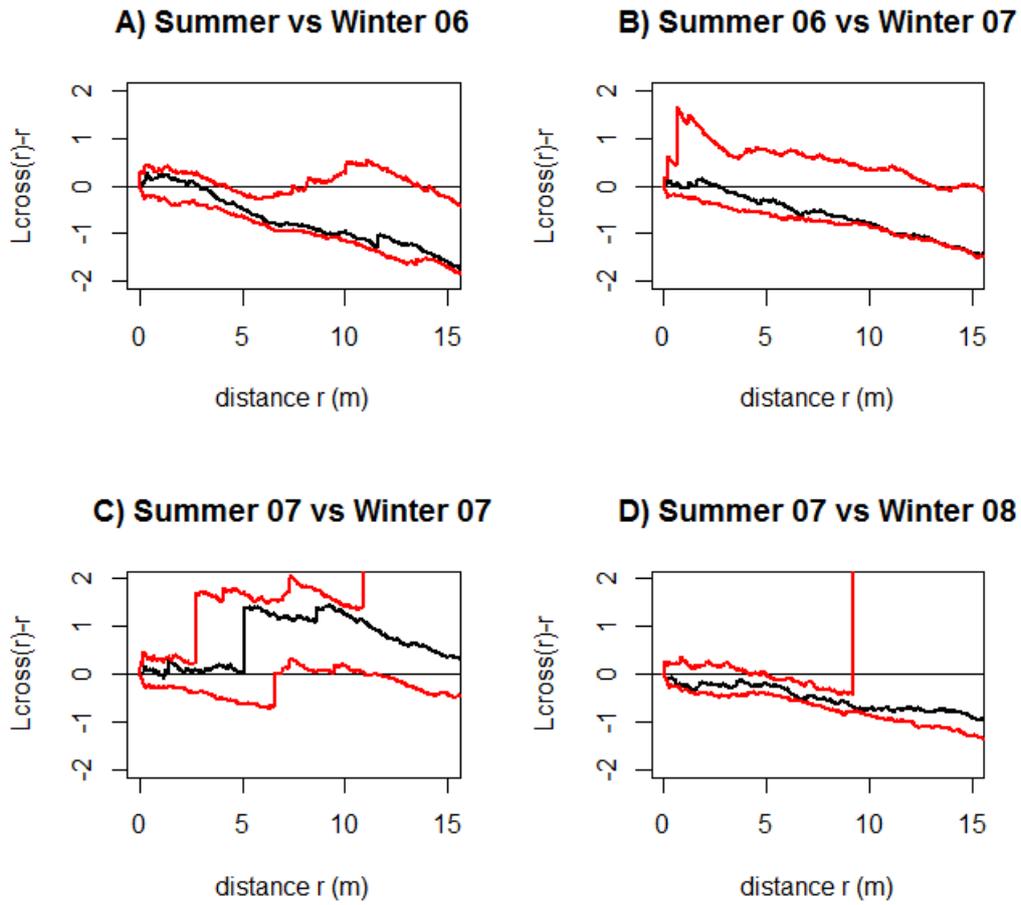
Figure 8S. Cross-type L- functions computed between subsequent epochs of measurement (black-colored lines) considering the small erosion scars. The limits of confidence envelope at level of 2% associated to the "population independence" hypothesis are calculated considering 99 random shifts in a rectangular window of a 2.5 m x 2.5 m.
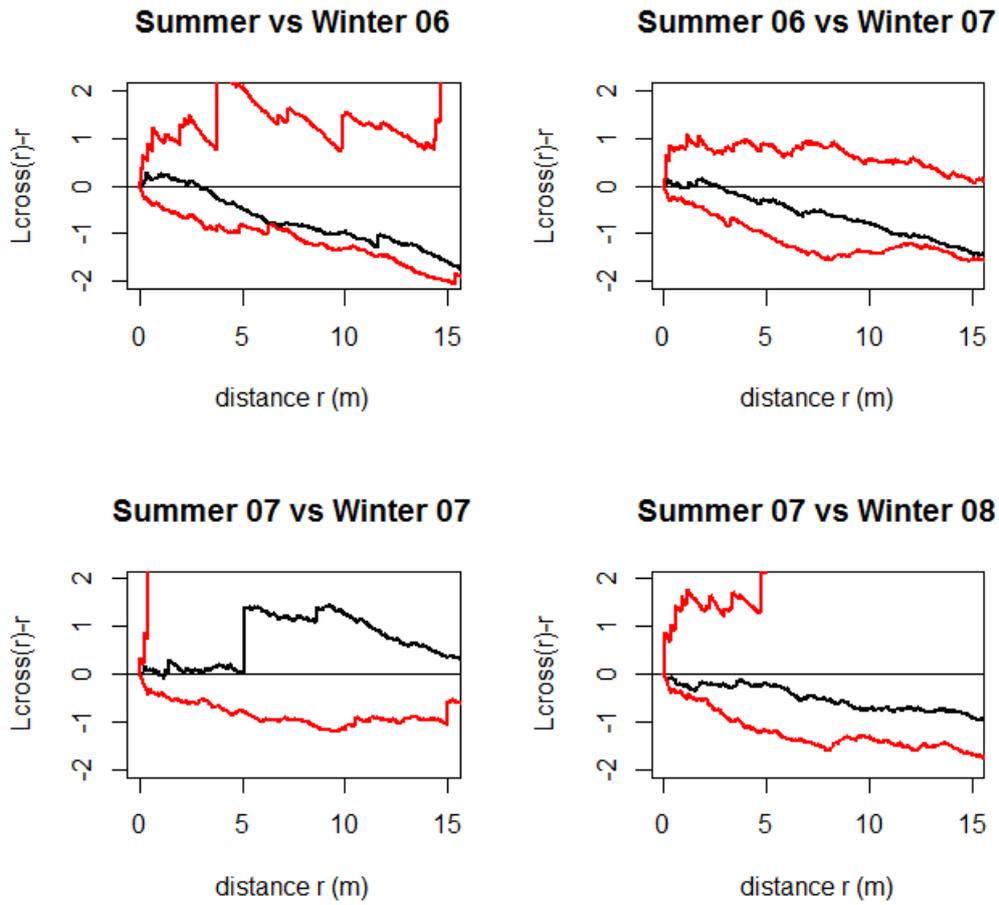
Figure 9S. Cross-type L- functions computed between subsequent epochs of measurement (black-coloured lines) considering the small erosion scars. The limits of confidence envelope at level of 2% associated to the "population independence" hypothesis are calculated considering 99 random shifts in a rectangular window of a 10 m x 10 m.
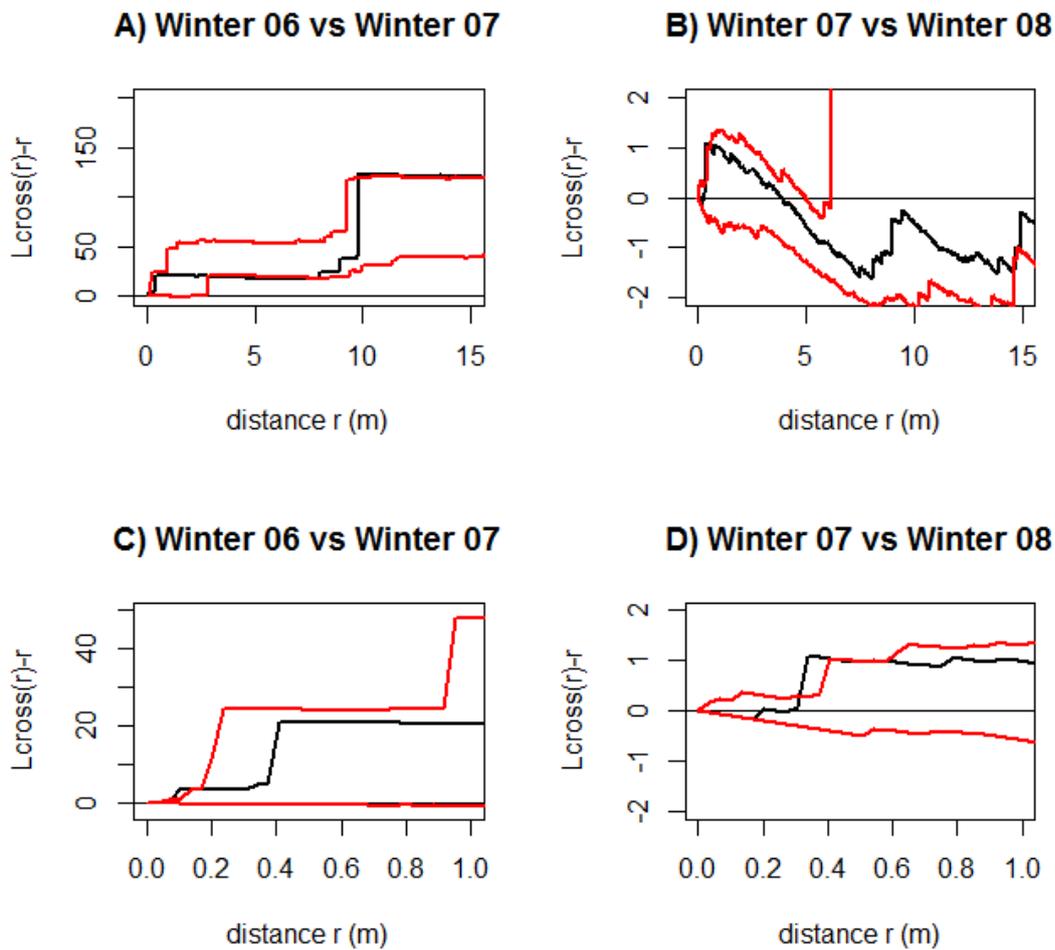
Figure 10S. Cross-type L- functions computed between subsequent epochs of measurement in winter (black-coloured lines) considering the large erosion scars. Figures C and D respectively correspond to a zoom on the distance range from 0 to 1.0 of Figures A and B. The limits of confidence envelope at level of 2% associated to the "population independence" hypothesis are calculated considering 99 random shifts in a rectangular window of a 2.5 m x 2.5 m.
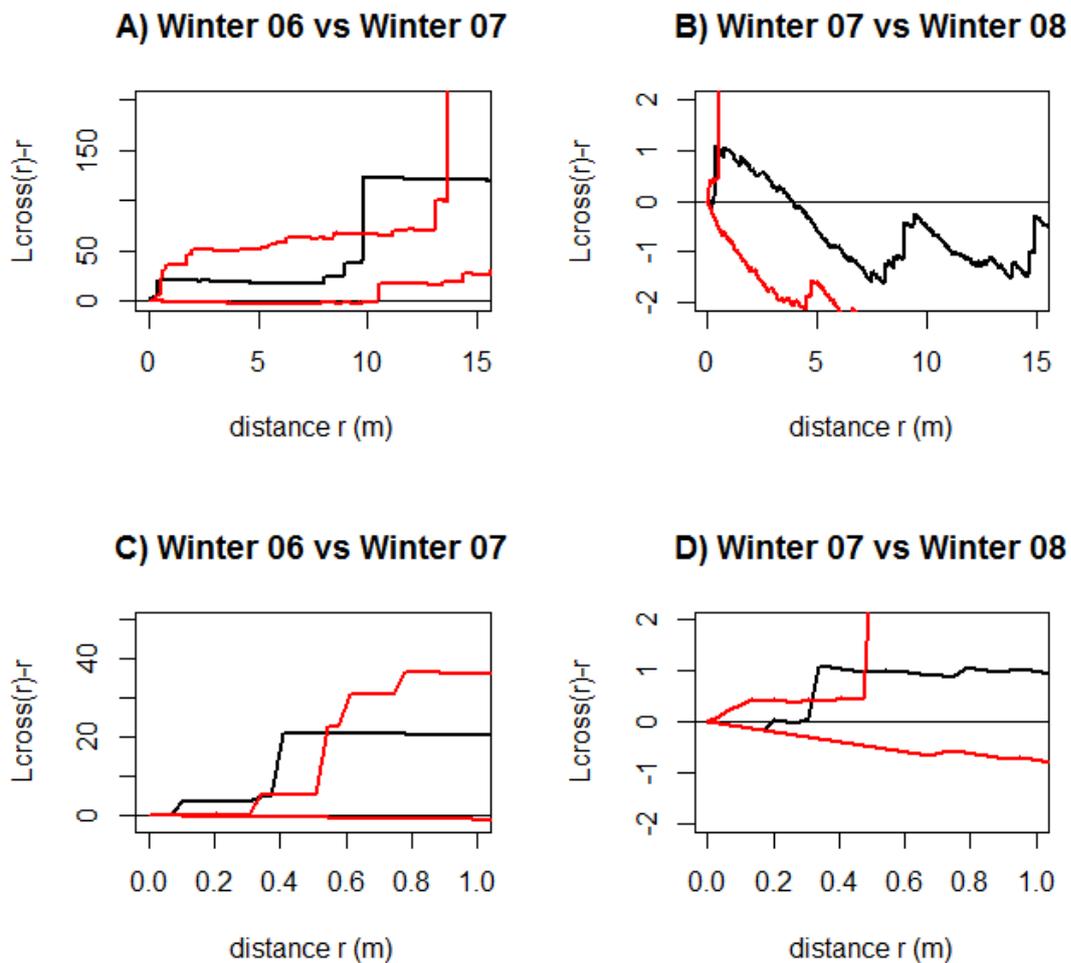
Figure 11S. Cross-type L- functions computed between subsequent epochs of measurement in winter (black-coloured lines) considering the large erosion scars. Figures C and D respectively correspond to a zoom on the distance range from 0 to 1.0 of Figures A and B. The limits of confidence envelope at level of 2% associated to the "population independence" hypothesis are calculated considering 99 random shifts in a rectangular window of a 10 m x 10 m.